

Design of a High-Temperature Test Facility for an Additive Manufactured Supercritical Carbon Dioxide Turbine

Anthony Grotjan PhD Student University of Wisconsin Madison, WI	Gregory Nellis Professor University of Wisconsin Madison, WI	Mark Anderson Associate Professor University of Wisconsin Madison, WI
--	---	--



Tony Grotjan is a Graduate Research Assistant working at the University of Wisconsin-Madison's Solar Energy Laboratory and Thermal Hydraulics Laboratory. His research is in supercritical carbon dioxide power cycle simulation, analysis, and development. His work focuses on the integration of turbomachinery loss modeling in the context of cycle design as well as turbomachinery experimentation with the goal of characterizing supercritical carbon dioxide cycles and turbomachinery to inform future generations of heat to power solutions.



Professor Nellis has engaged in research that builds on his expertise in cryogenics, refrigeration, heat transfer, thermodynamics, and energy systems. Professor Nellis received the R.W. Boom Award in 2008 from the Cryogenic Society of America and was elected a Fellow of ASHRAE in 2013. He co-authored the second edition of the book *Cryogenic Heat Transfer* which is widely used in the industry. He has received "Distinguished Professor" awards from the engineering student organizations Polygon and Pi Tau Sigma several times. Professor Nellis, together with his colleague Professor Sanford Klein, have co-authored three undergraduate-level texts and a reference book.



Dr. Mark Anderson is a Professor in the Department of Mechanical Engineering and Director of the University of Wisconsin's Thermal Hydraulic Laboratory. He also manages the UW-Madison Tantalus facility in Stoughton, WI. Dr. Anderson studies the physics, thermal hydraulic performance, and material corrosion issues of several different fluids (salts, liquid metals, SCW, sCO₂). He is also currently the U.S. representative to the International Atomic Energy Agency (IAEA) for the coordinated research project on supercritical fluids and has active research on the sCO₂ Brayton cycle for nuclear, solar, and fossil advanced power generation. He is one of the UW's Co-PIs on the Department of Energy fluoride-cooled nuclear reactor integrated research project and focuses on salt chemistry, purification, and materials compatibility. Dr. Anderson was recently awarded the Young Investigator Engineering Achievement Award from the American Nuclear Society for his work on liquid salts and supercritical fluids. He has been awarded three patents and has published over 150 papers in various areas related to physics, energy science, production, and utilization. Dr. Anderson currently serves as an Associate Editor for the ASME Journal of Nuclear Engineering & Radiation Science.

ABSTRACT

The supercritical carbon dioxide ($s\text{CO}_2$) power cycle has the potential to provide higher heat to power conversion efficiencies in combined heat and power applications than competing technologies. However, very high turbine inlet temperatures are required to achieve high thermal efficiency; the Department of Energy's target of 65% efficiency will require turbine inlet temperatures approaching 1300°C . Further metallurgical advancements as well as the development of complex turbine and generator cooling systems are required to reach these targets.

Additive manufacturing of turbine systems using advanced nickel-based super-alloys such as Haynes 282 has the potential to allow for higher temperature operation, and also provides design flexibility, addressing both material and cooling design challenges. A critical step in this advancement of supercritical carbon dioxide turbomachinery is the development of test facilities that can be used to characterize and validate the performance of novel turbine-generator system designs enabled by additive manufacturing.

A turbine test facility has been designed and is being fabricated that can achieve turbine inlet conditions of 800°C and 11 MPa, with a flow rate of 0.43 kg/s. The facility manages the complex auxiliary cooling flow requirements of high-temperature turbomachinery, allowing the test of various components in an advanced $s\text{CO}_2$ cycle. A 30 kW turbine-generator system that is additively manufactured using Haynes 282 with advanced cooling channel designs is being fabricated by an industry partner for installation in this facility. The performance of this turbine-generator system will be demonstrated while also studying the leakage and windage losses for small-scale supercritical carbon dioxide turbomachinery in order to calibrate modeling efforts used to develop a path towards higher efficiency cycles as metallurgical advancements continue to enable higher temperature operation. Additionally, insight is provided into the challenges associated with facility design as higher turbine inlet temperatures and larger scales are pursued.

INTRODUCTION

The advancement of clean, sustainable energy conversion and industrial decarbonization requires the development of more efficient power cycle technologies. One pathway to better heat to power conversion efficiencies is the development of the supercritical carbon dioxide power cycle as an enabling technology. With sufficiently high turbine inlet temperatures, the Recompressed Closed Brayton Cycle (RCBC) has the potential to achieve the Department of Energy's target cycle efficiency of 65%. Figure 1a shows a projection to this target at a turbine inlet temperature of 1300°C leveraging advancements in turbine technology enabling higher temperature operation. These projected cycle efficiencies are beyond the current state of the art and translate to annual energy savings on the order of quads in the United States alone as shown in Figure 1b.

The focus of the project that houses the present work is the turbine-generator component that is consistent with an advanced supercritical carbon dioxide cycle. This is the key piece of technology that is necessary to move the technology to higher efficiency and higher temperature. In addition, high rotational speeds and small turbomachine diameters are required to maintain high turbomachine isentropic efficiencies. While the small size of an $s\text{CO}_2$ turbine is

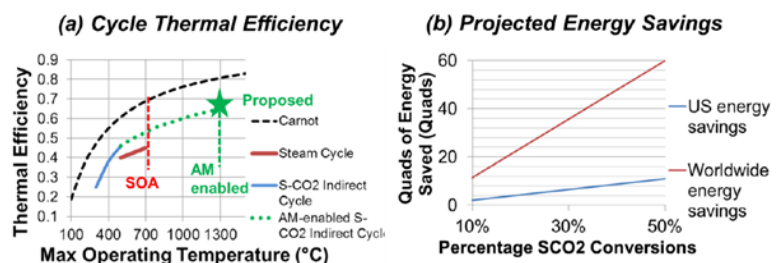


Figure 1: (a) Power generation cycle efficiency improvement enabled by proposed high-temperature turbine-generator technology, (b) potential per year energy savings due to efficiency improvement (Thoma)

usually considered to be an advantage, there are design challenges associated with internally cooled turbine blades as well as advanced generator technology.

Additive manufacturing of turbomachine technology has shown great promise in enabling high-temperature, high-speed operation based on its design flexibility for cooling channels and advantageous material properties at high temperatures. Haynes 282 is a nickel-based super-alloy with high strength and creep resistance at high temperatures. Additive manufacturing of turbomachinery from super-alloys like Haynes 282 and others still under development provides a path towards high-efficiency cycle operation, but these technologies are still emerging and require experimental validation.

For this reason, this paper describes a turbine test facility that has been commissioned to test a 30 kW turbine-generator system that will be additively manufactured using Haynes 282 with advanced cooling channel designs. The test facility has been designed to meet turbine inlet conditions of 800°C and 11 MPa, with a flow rate of 0.43 kg/s while managing the complex auxiliary cooling flow requirements associated with a high-temperature turbine. This facility will be used to validate the aerodynamic performance of the turbine, characterize the leakage and windage under high-speed operation at 80 kRPM, and evaluate the machine’s ability to survive under extreme operational conditions. The purpose of the present work is to describe the turbine test facility with a focus on the unique challenges associated with its extreme operational conditions.

RESULTS AND DISCUSSION

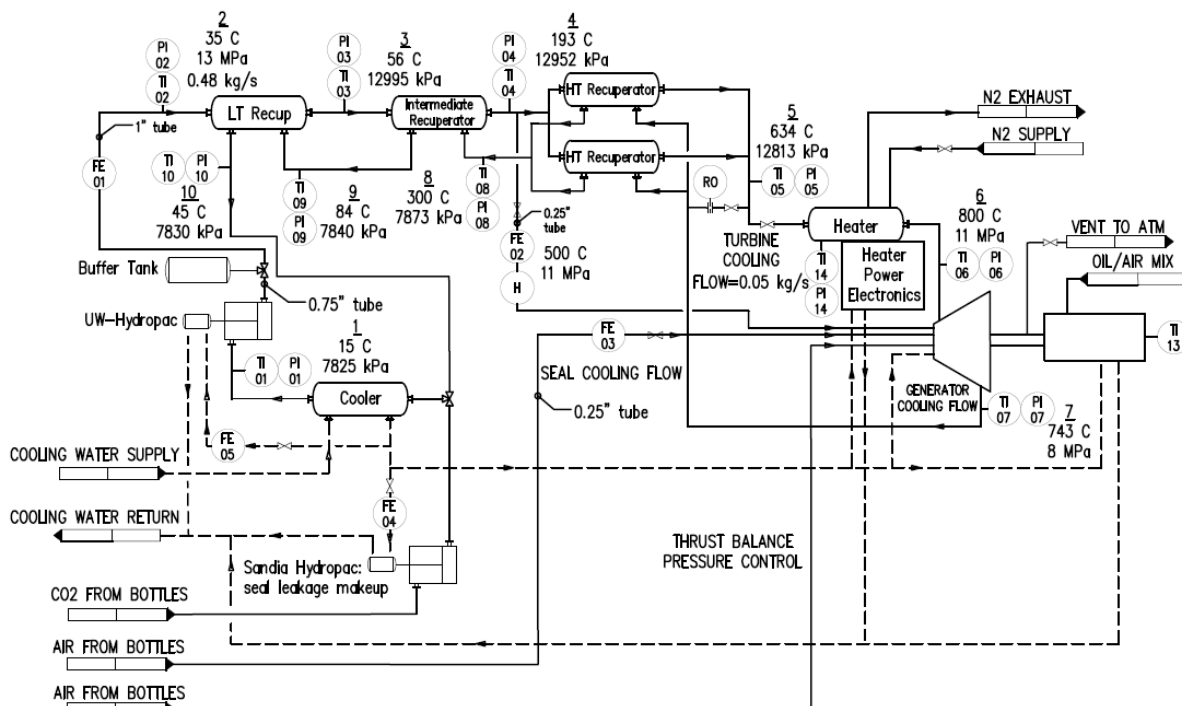


Figure 2: Turbine test facility schematic with thermodynamic states

The test loop is schematically shown in Figure 2. The steady state design point thermodynamic conditions are labeled for each state between components. A 3D rendering of the test facility is shown in Figure 3. The temperature-entropy diagram shown in Figure 4 locates each of the state points. It should be noted that state 7 represents the turbine outlet considering both the expansion process and mixing with cooling flow.

The present work describes the overall system design and component design and selection. The description of standard components is brief and instead the paper focuses on the more novel designs and challenges. Details related to the turbine-generator system itself are not given as this was designed and is being constructed by an industry partner, Raytheon Technology Research Center (RTRC), and is currently considered proprietary.

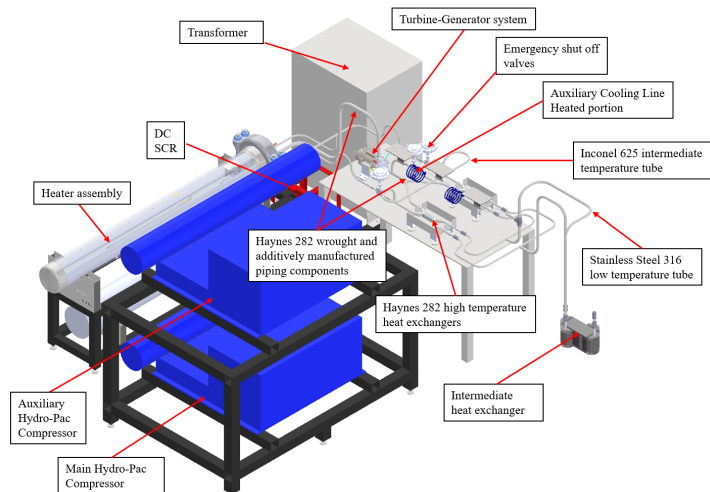


Figure 3: 3D representation of turbine test facility

Compressor

The overall flow and pressure rise requirements for the facility could be met by an existing single-stage, dual-piston Hydro-Pac LX compressor at the UW-Madison Thermal Hydraulics Laboratory (THL). The required system flow rate of 0.48 kg/s has been confirmed in previous tests under conditions where the inlet fluid is at a sufficiently high density at liquid conditions while also achieving a sufficient pressure rise and maintaining supercritical pressure conditions throughout the loop.

Since the Hydro-Pac is a reciprocating compressor, unavoidable pulsations in pressure and flow occur throughout the system. Data were collected at a high sampling rate (relative to the compressor frequency) in order to characterize the pulsations that are likely to be present at the turbine inlet. While pressure fluctuations are significant at the exit of the compressor, the peak-to-peak pressure variation can be attenuated to an acceptable level through the combination of the unavoidable pressure drop in the system between the compressor and the turbine as well as the installation of an appropriately sized buffer volume.

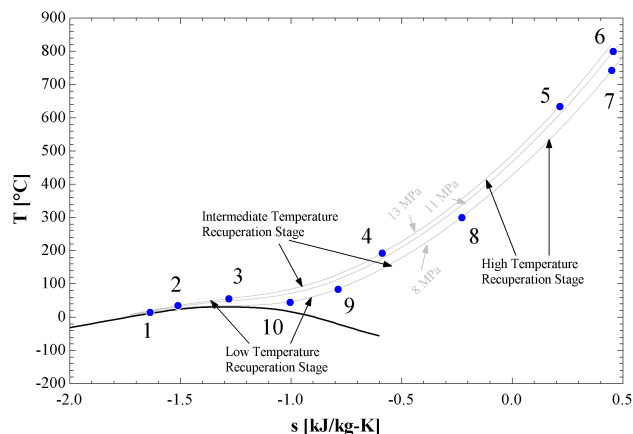


Figure 4: Temperature entropy diagram of test facility at steady state design conditions

Based on these studies, the pressure and flow variations are not expected to exceed 1% of the nominal mean values at the turbine inlet. The implications of this variation are discussed later in the context of system dynamics.

Cooler

To achieve the needed compression and flow, it was necessary to provide heat rejection so that the carbon dioxide achieved a low-temperature, incompressible state. A large, brazed-plate heat exchanger was purchased to be used as the testbed cooler. The goal was to cool carbon dioxide from 50°C to 15°C using chilled facility water available at 10°C flowing at approximately 40 GPM. These requirements translate to a required conductance of 6.1 kW/K and a heat transfer rate of 100 kW. An oversized, 60 brazed-plate model from Alfa Laval was selected with an on-design conductance of 7.70 kW/K and capacity to cool 122 kW with a pressure drop of 3.7 kPa on the carbon dioxide side and 30.1 kPa on the water side.

Recuperators

The carbon dioxide exiting the compressor must be heated to the turbine inlet temperature of 800°C. To minimize the required heat input to the cycle, several stages of recuperation were incorporated to achieve a total of 5.5 kW/K of on-design recuperation conductance. At design conditions, the flow exiting the turbine is still at a very high temperature in excess of 740°C. This provides opportunity for significant internal recuperation, but the high temperatures pose a material challenge. Few materials are rated for extended operation under pressure at temperatures near 800°C, as creep considerations are significant at elevated temperatures. Recuperators for high-temperature operation was the subject of research in a previous project conducted in the THL also in partnership with RTRC. Details of this project are described in further detail by Kuhr et al (Kuhr). Like the turbine system in the present work, the recuperator designed and tested in this previous project was additively manufactured from Haynes 282 in order to withstand extreme conditions of up to 800°C and pressures up to 250 bar. RTRC has provided two of these high-temperature, additive-manufactured recuperators for use in the present work. These are to be used in parallel to avoid excessive pressure drop.

These recuperators cover the most challenging temperature regime of recuperation, but further recuperation is required to minimize the external heating and cooling required. The described high-temperature solution is therefore combined in series with a brazed plate heat exchanger from Alfa Laval, which provides significant conductance at a reasonable cost. This was the same model as the heat exchanger used for the cooler and helps cover the challenging temperature regime of recuperation near the vapor dome at low temperatures without contributing a large pressure drop. While the duty and temperature difference provided by this heat exchanger are comparatively low, this recuperation stage provides the majority of the conductance as the cold regime approaches the vapor dome where the temperature profiles flatten and the pinch point exists as can be seen from states 2 to 3 and 9 to 10 in Figure 4.

The brazing of the low-temperature heat exchanger has a temperature limitation of 150°C, motivating the need for an intermediate stage of recuperation between this and the high-temperature,

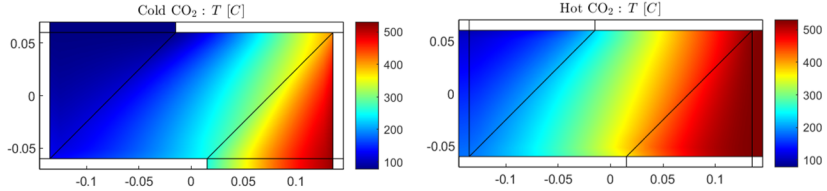


Figure 5: Custom-designed diffusion bonded PCHE – simulated stream temperature distributions from top view for cold stream (left) and hot stream (right)

additive-manufactured recuperators provided by RTRC. To cover the intermediate temperature range, a stainless steel 316, diffusion-bonded, Printed Circuit Heat Exchanger (PCHE) was custom-designed based on correlations studied within the THL. Details of the heat transfer correlations and PCHE design and analysis methods developed at the THL and used in this design are described by Jentz et al (Jentz). The intermediate temperature PCHE was designed using zig-zag channels with alternating hot and cold plates. Of the 94 channeled plates, 32 are channeled for the cold stream, while 62 are channeled for the hot stream. Two hot plates were used between cold plates to reduce the pressure drop on the hot side of the PCHE. Figure 5 shows a map of the temperatures for the cold and hot streams as simulated using the modeling infrastructure available in the THL. Table 1 summarizes the specifications of each stage of recuperation under steady state design operation.

Table 1: Specifications of heat transfer duty, conductance, effectiveness, inlet and exit temperatures for each stream, and pressure drop of each stream for each stage of recuperation. Note that the high-temperature recuperation stage includes two heat exchangers in parallel.

Stage	\dot{Q} [kW]	UA [kW/K]	ϵ	$T_{C,in}$ [°C]	$T_{C,out}$ [°C]	$T_{H,in}$ [°C]	$T_{H,out}$ [°C]	ΔP_C [kPa]	ΔP_H [kPa]
Low	35	2.50	0.72	35	56	84	45	5	10
Int.	125	1.86	0.86	56	193	300	84	43	33
High	125	1.13	0.81	193	634	743	300	139	127

Heater

After recuperation, 120 kW of heat input is still required to reach the target turbine inlet temperature of 800°C. Direct electrical resistance heating is used in the experimental facility by applying a current to a tube containing flowing carbon dioxide. While this provides a safe and clean method, the design of the heater represented significant material and mechanical challenges associated with high-temperature power cycle operation due to the competing requirements of mechanical pressure containment and electrical resistance. As metal temperature increases, its strength decreases making it difficult to contain the necessary high internal pressure. This is especially true above 600°C as creep becomes a major issue at elevated temperatures.

While this would usually lead to the use of a thick-walled pipe to compensate for lack of inherent material strength, the need for high electrical resistance prevents this approach. In order to draw a current achievable in the laboratory facility, a high electrical resistance is required. The electrical resistance of the heater tube is proportional to the resistivity of the material and the length of the tube, and inversely proportional to the cross-sectional area of the tube. There is a limit on increasing the length of the tube imposed by pressure drop considerations and therefore, it is necessary to use a thin-walled tube. To account for the resulting low strength at high temperatures, the heater tube is enclosed and sealed in a pressure vessel that is filled with inert nitrogen exerting an external pressure on the heater tube to balance the internal loading from the flowing carbon dioxide. Supply and exhaust ports in this volume are controlled by pneumatically actuated valves to nearly match measured pressure inside the heating element.

The heating element is constructed from Inconel 625 tube with an outer diameter of 0.5", a wall thickness of 0.028", and a length of 23.3 ft. Flow through this tube results in a pressure drop of 1800 kPa. The heating element sits in

an insulation tray filled with powder insulation so that the external pressure vessel does not need to withstand high temperatures. The pressure vessel is constructed from API 5L X65 NPS 10" SCH40 pipe capped with a blind Grayloc flange. Figure 6 shows a 3D model of the heater assembly without the outer pressure vessel for visibility of internal components.

To meet the heating requirements, a current of 710 A is applied to the heating element. To maximize the output DC current from the laboratory facility 480 VAC, 200 A source, a combination of power electronics was selected for conversion and rectification. A 300 kVA, 600 to 208V transformer was purchased to transform the electrical input to a higher current. Even though the laboratory facility input is 480 VAC, a 600 VAC primary side transformer was selected to maximize the conversion ratio and therefore maximize the output current. The transformer is wired in series to a DC Silicon Controlled Rectifier (SCR), made by Energy Research Associates and already owned by the THL, which rectifies the AC input to a single, DC output. A schematic of the power electronics system is shown in Figure 7.

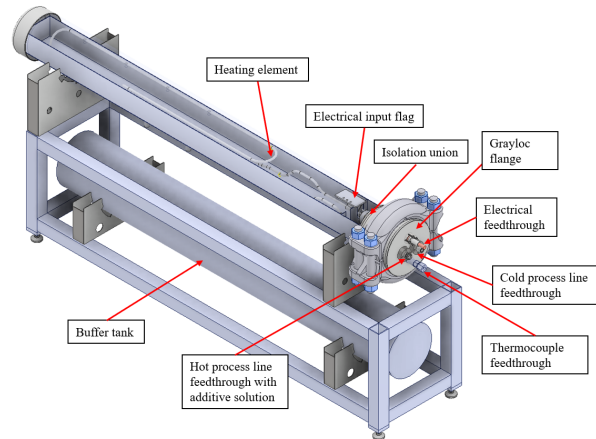


Figure 6: 3D model of heater assembly design with outer pressure vessel hidden for visibility of internal components

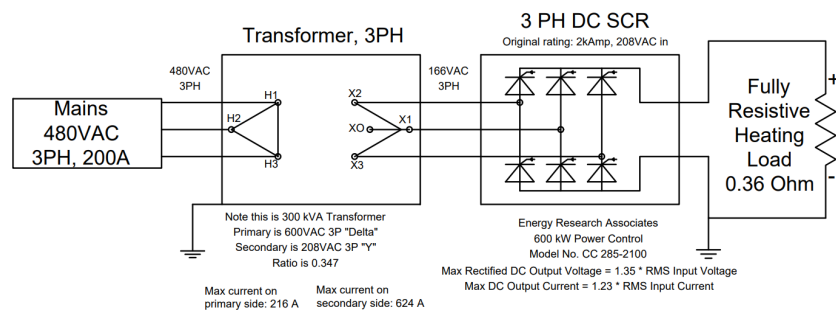


Figure 7: Heater power supply schematic

There are a number of feedthrough passages required through the pressure boundary of the high-temperature heater. For brevity, only the process line feedthrough is discussed as a representative example of high-temperature design challenges associated with these feedthroughs.

A feedthrough for the carbon dioxide process lines was designed and manufactured at UW. This was designed using Mandatory Appendix 2 – “Rules for Bolted Flange Connections with Ring Type Gaskets” of Section VIII Division 1 of the ASME Boiler and Pressure Vessel Code (ASME).

Figure 8 shows a diagram of the cold side process line feedthrough assembly. The bolted flange clamps down on the graphite seal while a sleeve containing pourable insulation limits the conductive path from the hot process line to the graphite seal and the dissimilar weld between Inconel 625 and Stainless Steel 316 in order to limit thermal stress induced by differences in thermal expansion.

Note the location of pressure balancing along the process line tube as it feeds into the heater pressure vessel. The pressure vessel interior is on the left side of the Grayloc flange, while the surroundings are on the right. Because of the seal and weld locations that form the pressure boundary, the region containing the pourable insulation for thermal isolation exists at surrounding pressure conditions and therefore provides no pressure balance along much of the length of the 3/4” feedthrough tube. While the strength is sufficient at the cold inlet of the heater, the pressure imbalance is an issue on the 800°C hot exit.

Like many of the high-temperature components of this project, an additive manufactured Haynes 282 solution was implemented to resolve this. Figure 9 shows the hot side feedthrough, which leverages the strength at high temperature available with Haynes 282 as well as the design flexibility of additive manufacturing to increase the wall thickness. A portion of the thermal isolation sleeve was manufactured from Haynes 282 to provide a thermal standoff so that the dissimilar welds at material transitions occurred at reasonably low temperatures. The colors in Figure 9 emphasize material transition.

After the process line passes through the pressure boundary, the electrical current must pass into the heating element while remaining isolated from the incoming 3/4” OD process line. This is accomplished with a custom-designed isolation union made primarily from Inconel 625 and shown in Figure 10.

This flange had the unique challenges of requiring a sealed connection at a design temperature of 650°C while also providing electrical iso-

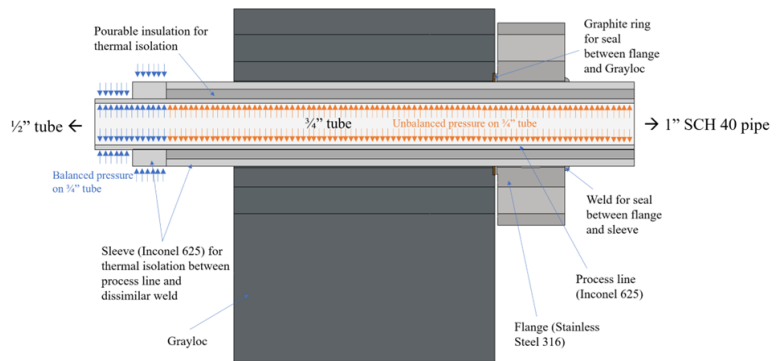


Figure 8: Cold side process line feedthrough assembly with annotated pressure imbalance

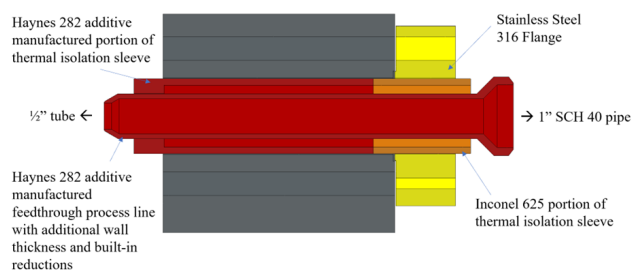


Figure 9: Hot side process line feedthrough assembly using additive manufactured solution. Colors for material transition emphasis (red: additive manufactured Haynes 282, orange: Inconel 625, yellow: Stainless Steel 316).

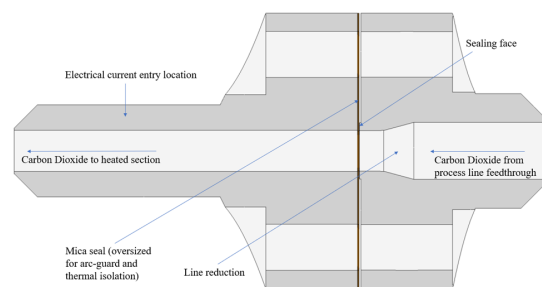


Figure 10: Isolation union assembly design

lation so that all of the current passes into the heated portion (to the left in Figure 10), and not out of the pressure vessel (to the right on Figure 10). Graphite is electrically conductive and its temperature rating is significantly below the design temperature, making it not suitable. Instead, mica was proposed as a sealing material. The properties of mica as a sealant were not well known, so its suitability as a seal was experimentally confirmed at design loading. While not as compliant as graphite or other conventional sealing materials, experimentation and scaling analysis predict sufficiently small leak rates for this design.

Auxiliary Requirements for Turbine Operation

An auxiliary cooling line is required to cool the turbine blades using carbon dioxide pulled off from the main flow of the test loop to provide the required 0.05 kg/s of carbon dioxide at 500°C and 11 MPa. An auxiliary heater was developed to bring carbon dioxide from before the high-temperature heat exchangers (state 4 in Figure 2) from 193°C up to 500°C. With this configuration, it is feasible to use a Coriolis flow meter to measure the flow rate before heating. This is a coiled, direct heating solution made from ¼" OD, 0.035" WT stainless steel 316 tube.

The turbine design specifies a seal leakage of 0.02 kg/s. Recycling of the leaked carbon dioxide into the loop was originally considered, but the required low turbine cavity pressure along with the potential for oil from the lubrication system to enter the main flow were factors in the decision against recycling of leakage. Instead of using an additional compressor to recycle and pump down the turbine cavity, it was instead decided to exhaust the leakage and use an additional compressor to make up the leakage from a carbon dioxide inventory associated with a manifold of bottles. Sandia National Labs has provided an additional Hydro-Pac LX compressor for this purpose. While the required make up flow is small, there is a high pressure rise required to bring additional carbon dioxide from a supply manifold of bottles up to supercritical conditions, warranting the need for another large compressor.

Emergency Shut-down Transients

To protect the turbo-generator from overspeed in case of a loss of load event, turbine bypass valves have been identified to quickly divert flow around the turbo-generator. If an overspeed event is detected, the valves will actuate to bypass the turbo-generator. Pneumatically actuated valves with a measured shutoff time of 1/30 second have been identified as a solution. Two of these valves will be placed in the normally open configuration before the heater to reduce pressure drop, while a third will be normally closed and positioned to bypass the heater and turbine when opened. These valves are all rated for 135 MPa and 650°C.

In the case where no action is taken to shut down carbon dioxide flow and the turbine is allowed to accelerate in the absence of generator loading, there is a plateau in the rotational speed that will be achieved because of the reduction in aerodynamic efficiency that occurs with increasing speed. Figure 11 shows the turbine aerodynamic efficiency dropping as a result of this speed-up, causing the limit on acceleration and leading to a plateau in speed in a matter of approximately 3 seconds.

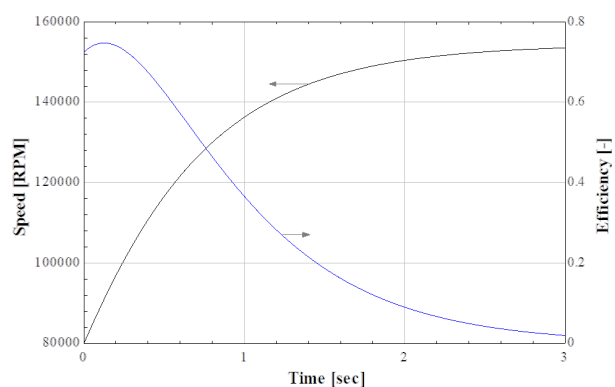


Figure 11: Unconstrained turbine acceleration in absence of generator loading

The critical overspeed to avoid was determined by considering bearing limitations, critical modes, information from the manufacturer, and standards in the literature. Bearing specifications indicate a limit of 97 kRPM, which was consistent with the American Petroleum Institute standard, API 670 (*Machinery Protection Systems*), which specifies avoiding a 121% overspeed of 96.8 kRPM. A limit of 96.8 kRPM has been chosen as an overspeed limit specification based on these considerations.

A transient blowdown analysis was conducted for the system consisting of the remaining volume downstream of the emergency shutoff valves, which includes the heater and connecting pipes as shown in Figure 2. The main intent of this analysis was to determine the emergency shutoff procedure necessary to avoid overspeed failure in the worst-case scenario of losing all ability to apply a braking torque from the generator electronics. The method was to couple an angular momentum balance with a mass balance and an energy balance. These coupled balances were numerically integrated through time to determine when the turbine would reach a critical failure speed. Each case considered here conservatively neglects bearing friction and windage, so there is no term to work against the acceleration of the turbine in the emergency case of lost generator torque.

The initial acceleration during the shutoff valve mechanical delay is consistent with the unconstrained acceleration shown in Figure 11. The following blowdown regime significantly shortens the acceleration process, not relying on turbine efficiency reduction to halt acceleration. Once exhaust through the remaining blowdown volume is complete and pressure equilibrates across the turbine, no further flow drives the turbine, resulting in a plateau in speed (for this case where losses are neglected). When beginning at an initial condition corresponding to the steady state operating speed of 80 kRPM, the resulting plateau speed is far lower than critical failure at 90.4 kRPM. Figure 12 shows the results of the transient analysis starting at steady state conditions. It is advisable to avoid prematurely triggering the emergency shutoff routine as to avoid unnecessary stress on the system. The initial condition that results in the overspeed limit of 96.8 kRPM was determined to be 87 kRPM. Figure 13 shows the results of the transient analysis starting at the decided upon emergency procedure triggering speed of 87 kRPM.

The described analyses were conducted assuming constant inlet thermodynamic conditions, but due to the reciprocating nature of the Hydro-Pac compressor driving the flow, pressure and flow pulsations are expected as described in the Compressor section. Analysis was conducted to determine the pulsation limitations based on the generator torque limit of 3 N-m. Initial calculations indicate that a pressure pulsation of approximately 5% of the nominal mean value at the turbine inlet can be tolerated without exceeding the maximum torque the generator can produce to control the turbine speed. This provides an acceptable margin compared to the expectation of 1%.

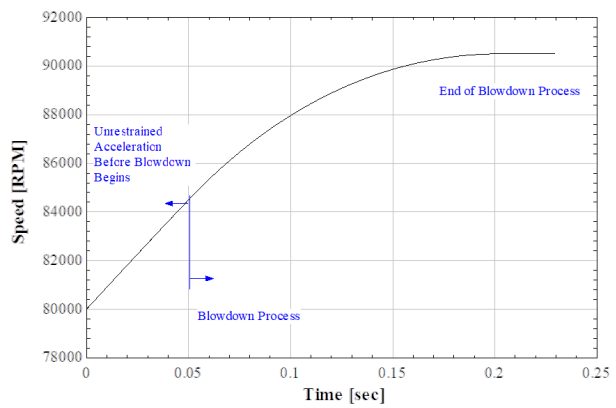


Figure 12: Turbine acceleration in absence of generator loading during emergency shutoff procedure starting at 80 kRPM steady state condition

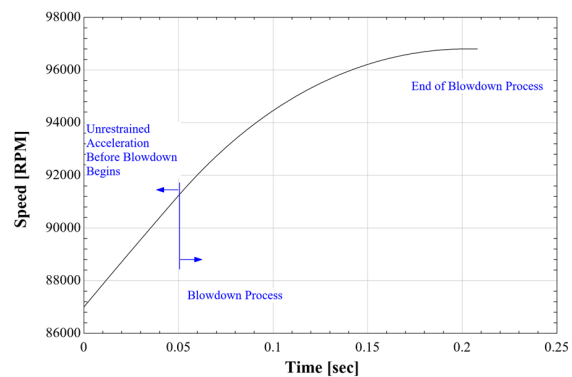


Figure 13: Turbine acceleration in absence of generator loading during emergency shutoff procedure starting at 87 kRPM and ending at critical limit

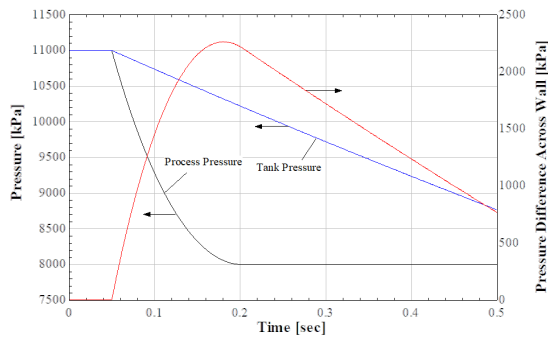


Figure 14: Pressure inside and outside heating element during transient emergency process with common initial condition

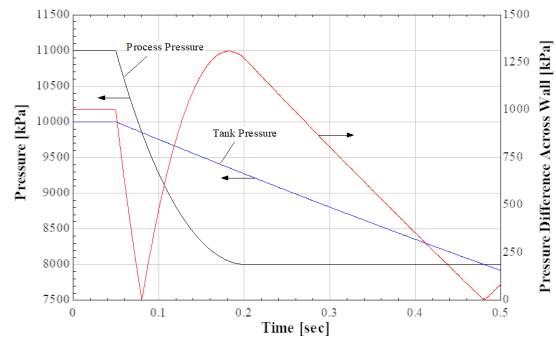


Figure 15: Pressure inside and outside heating element during transient emergency process with offset initial condition

An additional consideration related to the emergency shutoff procedure is the exhausting of nitrogen from the heater pressure vessel. Recall that the vessel will be filled with nitrogen at a pressure nearly matching the carbon dioxide pressure inside the thin-walled resistive heating element to minimize the load across the wall. The exhausting of this vessel has a much larger time constant compared to the transients described above. As a result, the pressure difference across the wall briefly exceeds the maximum rated pressure difference for this tube, which is approximately 2000 kPa at operating temperature according to ASME boiler and pressure vessel codes. This effect is shown in Figure 14.

To remedy this issue, the steady state tank pressure will operate at an offset pressure 1 MPa lower than the process pressure. This gives the nitrogen exhausting process a head start compared to the process carbon dioxide exhausting through the turbine in the case of a shut-down event as shown in Figure 15.

Conclusion

A turbine test facility has been designed and is being fabricated that can achieve turbine inlet conditions of 800°C and 11 MPa, and with a flow rate of 0.43 kg/s. Each of the components described in this design summary has been procured or constructed. Assembly of the turbine test facility is currently underway with the expectation of receipt and testing of an advanced turbine-generator system that is additively manufactured by our industry partner using Haynes 282 with advanced cooling channel designs. Many challenges were encountered in the design of this facility, particularly in the design of components in the high-temperature region of the cycle, and the control and overspeed protection of a turbomachine spinning at 80 kRPM. This summary has provided insights into the design solutions associated with these challenges. The objective of the test facility is to validate the performance of this and other novel turbomachinery as a step toward high-temperature, high efficiency power cycles of the future.

REFERENCES

- Machinery Protection Systems*. Standard. American Petroleum Institute, Nov. 2014.
- ASME. *ASME Boiler and Pressure Vessel Code: Section VIII, Division 1, Mandatory Appendix 2 – “Rules for Bolted Flange Connections with Ring Type Gaskets”*. American Society of Mechanical Engineers, 2006.
- Jentz, Ian. “Thermohydraulic and Mechanical Modeling of Printed Circuit Heat Exchangers for Next Generation Nuclear Service”. PhD thesis, University of Wisconsin-Madison, 2021.
- Kuhr, Dane. “Performance Characterization of Compact Heat Exchangers within a Supercritical Carbon Dioxide Brayton Cycle”. MA thesis, 2022.
- Thoma, Dan et al. *Additive Manufactured Supercritical CO2 Heat to Power Solution*. Tech. rep. University of Wisconsin-Madison, Madison, WI (United States), 2019.

ACKNOWLEDGEMENTS

This material is based upon work supported by the Department of Energy - Industrial Energy and Decarbonization Office under the Award Number DE-EE0009138.